Unriddling the role of alkali metal cations and Pt-surface hydroxide in alkaline hydrogen evolution reaction

Aamir Hassan Shah[1], Zisheng Zhang[1], Zhihong Huang[2], Sibo Wang[1], Guangyan Zhong[1], Chengzhang Wan[1,2], Anastassia N. Alexandrova[1], Yu Huang[2,3], Xiangfeng Duan[1,3,*]

[1]*Department of Chemistry and Biochemistry, University of California, Los Angeles; California 90095, United States.*

[2]*Department of Materials Science and Engineering, University of California, Los Angeles; California 90095, United States.*

[3]*California NanoSystems Institute, University of California, Los Angeles; California 90095, United States.*

[*]*Correspondence: xduan@chem.ucla.edu, yhuang@seas.ucla.edu, ana@chem.ucla.edu*

Sustainable production of hydrogen by water electrolysis is a promising pathway to cope with the growing demands for renewable energy conversion and storage. The alkaline electrolysis is attracting increasing attention for more facile anodic oxygen evolution reaction (OER) but plagued by poorer kinetics in cathodic hydrogen evolution reaction (HER) even with the platinum (Pt) catalysts. With the presence of alkali metal cations and hydroxyl anions, the electrode-electrolyte (Pt-water) interface in alkaline electrolyte is far more complex than that in acidic environment. Despite considerable efforts in probing the HER kinetics in alkaline electrolyte, the exact role of these different species remains elusive and represents a topic of considerable debate. Herein, we combine electrochemical impedance spectroscopy (EIS) and a unique electrical transport spectroscopy (ETS) approach to probe and understand the fundamental role of different cations (Li^+, Na^+ and K^+) in HER kinetics. The ETS approach provides a highly specific signaling transduction pathway to exclusively probe the surface adsorbates, while the EIS offers the critical information regarding the near surface environment in the electrical double layer (EDL). Based on these comprehensive *on-surface and near-surface* signals, our theoretical calculations with explicit solvation further help establish the molecular level insights into the surface adsorption properties, solvation structure, and Pt-water interface dynamics in presence of different cations and surface hydroxyl adsorbate (OH_{ad}). Our integrated studies

suggest that the alkali metal cations play an indirect role in modifying HER kinetics: with the smaller cations less destabilizing OH_{ad} in the HER potential window to favor a higher OH_{ad} coverage on Pt surface. The surface OH_{ad} is highly polar and acts as both electronically favored proton-acceptors and geometrically favored proton-donors to promote water dissociation in alkaline media, thus boosting the Volmer step kinetics and the HER activity. Our study resolves the elusive role of alkali metal cations and Pt-surface OH_{ad} in alkaline HER, and could offer valuable insights for the design of more efficient electrolyzers for renewable energy conversion.

The hydrogen evolution reaction (HER) is one of the most fundamental and critical reactions in renewable energy conversion and storage devices including electrolyzers that convert and store intermittent renewable electricity in chemical form by producing hydrogen. On the other hand, hydrogen oxidation reaction (HOR) plays a critical role in fuel cell technologies that converts stored chemical energy back to electricity. The HER/HOR mechanism and kinetics are drastically different in acidic and alkaline media[1,2]. Platinum (Pt) is state of the art electrocatalyst for these reactions and thus significant efforts have been invested in understanding the reaction mechanism and kinetics on Pt-based electrocatalytic systems[3-5]. Hitherto, various hypotheses have been proposed to identify and understand the reaction descriptors that account for the pH effect on HER on Pt electrode surfaces. It has been well-recognized that the HER rate and mechanism is related to the strength of metal hydrogen binding energy (HBE). In particular, Nørskov *et al.* have generated the volcano plot using density functional theory (DFT) database of hydrogen chemisorption energies on close packed surfaces of various transition and noble metals[4], and confirmed that Pt represents an optimum HER catalyst particularly in acidic environment.

Although the HBE of pure metal surface can in principle serve as an effective physical descriptor for HER, the experimental determination of the relevant physical parameters is often complicated by the presence of the electrolyte and different surface adsorbates, particularly in alkaline electrolytes where the adsorbates are more complex. For example, Yan *et al.* studied the HER in different pH-buffered electrolytes and suggested that monotonic decrease in HER activities by increasing the pH can be correlated with the continuously strengthened

electrochemical HBE values[6]. On the other hand, Koper and coworkers suggested that positive shift in the hydrogen underpotential deposition (H_{upd}) peak in cyclic voltammetry is not because of the HBE changes, but originates from destabilization of the hydroxyl adsorbates (OH_{ad}) on Pt(100) and Pt(110) sites by the presence of alkali metal cations near the interface[7,8]. Moreover, Koper *et al.* have also shown that the HBE descriptor cannot fully explain the pH dependent catalytic behavior on Pt(111) that shows significant pH dependent HER kinetics yet little pH dependent H_{upd} peak potential shift[9]. Thus, despite the undeniable success of the HBE in acidic media, it is not an unambiguous descriptor for HER/HOR kinetics in alkaline media, largely due to more complex electrolyte environment and the elusive role of different surface adsorbates that may modify the interfacial molecular structures and reaction pathways.

Markovic *et al.* ascribed the slower HER kinetics in alkaline media to the high energy barrier for H_2O dissociation as compared to the H_3O^+ in acidic media[10-12], and suggested that the HER kinetics in alkaline media can be improved by presence of oxophilic groups that can stabilize OH_{ad}, which in turn facilitates H_2O dissociation[13]. Later, the same group observed a monotonic relationship between HER activity and the OH_{ad} affinity of the oxophilic groups and concluded that the HER activity follows Brønsted–Evans–Polanyi principle to promote the HER kinetics and proposed a bifunctional mechanism—the edges of oxophilic metal clusters ($M(OH)_2$) promote the H_2O dissociation and production of H_{ad} on nearby Pt surfaces that then recombine into molecular hydrogen[14]. This bifunctional mechanism has been supported by a number of studies[15-18]. For example, Jia and coworkers experimentally verified the bifunctional mechanism by combined electrochemical and operando spectroscopic data[15], and robustly demonstrated that the presence of hydroxyl groups on surface Ru sites in the HOR potential region plays a key role in promoting the rate-determining Volmer step[15]. Moreover, Koper *et al.* recently further investigated the role of OH_{ad} on HER activity in alkaline media and demonstrated that HER activity exhibits a volcano-type relationship with the hydroxide binding strength, supporting Brønsted–Evans–Polyani relationship[19].

Beside HBE and bifunctional mechanism, Koper and coworkers suggested the potential of zero free charge (pzfc) may play an important role[9]. In this picture, the HER/HOR region in acidic media is closer to the pzfc (~0.34 V vs. RHE), and the reorganization energy of interfacial

water to move a proton through electrical double layer is small; while the HER/HOR region in alkaline media is far from the pzfc (~1.0 V vs. RHE, i.e. closer to the OH_{ad} region) and the strong electric field in HER/HOR region leads to a large interfacial water reorganization energy that could limit OH^- transfers through double layer[9].

Beside the differences in these distinct theories and different level of success in various aspects, none of them considered the effect of alkali metal cations (AM^+) on HER kinetics, which can hardly be ignored in alkaline electrolytes. For example, Markovic and coworkers observed promotional HER activity on $Ni(OH)_2$-Pt surface in the presence of Li^+ cations and attributed it to water dissociation[13]. Bandarenka and coworkers reported a similar promotion of HER activity on Pt electrode by cations[20], and suggested cations may alter the HBE, thus altering the HER activities[20]. Jia and coworkers attributed the enhancement in HER activity to presence of OH_{ad}-$(H_2O)_x$-AM^+ in the double-layer region, which facilitates the removal/transport of OH_{ad} into the bulk, forming OH^--$(H_2O)_x$-AM^+ as per the hard–soft acid–base theory, thereby promoting HER[16]. Koper et al. recently suggested a change in the rate-determining step from Heyrovsky to Volmer step in Li^+ and K^+ containing electrolytes, respectively[21]. Overall, **although the enhancement of HER activity on Pt electrode in presence of Li^+ when compared with other larger AM^+ has been consistently observed, a full understanding of this phenomenon has been a topic considerable debate.** Therefore, to more completely understand the descriptor that dictates HER activity in alkaline media, it is essential to investigate how the different cations alter the local (**on-surface or near surface**) chemical environment at electrode-electrolyte interface.

Here we address this issue by systematically studying the influence of cations on HER on Pt surface in alkaline media. We observed that the HER activity in alkaline media is clearly dependent on the exact AM^+ ($Li^+ > Na^+ > K^+$), which is consistent with previous studies[20,22]. We further exploit a unique electrical transport spectroscopy (ETS) approach to directly probe the Pt-surface adsorbates at variable potentials, and electrochemical impedance spectroscopy (EIS) to study the near surface environment in the electrical double layer (EDL) and charge transfer resistance at the electrode-electrolyte interface. Based on these comprehensive on-surface and near-surface signals, we conduct density functional theory (DFT) calculations with explicit solvation, including static calculation, grand canonical DFT calculation, *ab initio* molecular

dynamic (AIMD) simulation, and micro-solvation molecular cluster calculations, to develop molecular level insights into the surface adsorption properties, solvation structure, and the Pt-water interface dynamics in presence of cations and surface OH_{ad} species. Together, we experimentally and theoretically resolve the elusive role of AM^+, and demonstrates AM^+ plays an indirect role in modifying the adsorption strength and coverage of the hydroxyl species (OH_{ad}) ($-OH_{ad@Li+}$ > $-OH_{ad@Na+}$ > $-OH_{ad@K+}$) under the H_{upd}/HER potential regime, where the high OH_{ad} coverage with smaller AM^+ promotes the HER activity[23,24].

Specifically, our integrated studies reveal that Li^+ cations less destabilize OH_{ad} on Pt surface (than Na^+ and K^+) and help retain more OH_{ad} that in turn act as **both proton acceptors and donors** to the nearby water molecules and facilitate the Volmer step kinetics and the HER activity in alkaline media (similar to the "bifunctional mechanism"), as also confirmed by greatly reduced charge transfer resistance observed in EIS studies. Our direct experimental and theoretical evidences provide critical fundamental insights into how and why AM^+ influence the HER kinetics in alkaline media. It could enable an important vision for the design of future electrolyzers with improved energy efficiency and reduced cost.

Cation dependent HER activity and surface adsorbates

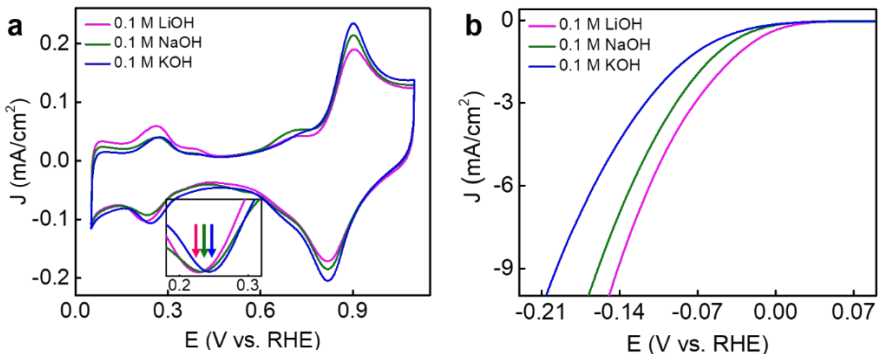

Figure 1| Voltammetric studies in alkali electrolyte with different alkali metal cations. (a) CV (inset shows zoomed-in view of the normalized H_{upd} peak) on stationary electrode at scan rate of 100 mV/sec. **(b)** IR-corrected HER polarization curves collected at room temperature on polycrystalline Pt disc electrode in N_2-saturated 0.1 M MOH (M= Li^+, Na^+ and K^+) at a scan rate of 5 mV/sec with rotation speed of 1600 rpm.

We have first examined the influence of cations by cyclic and linear scan voltammetry on Pt-disc electrode using conventional three electrode system in alkaline electrolytes at pH 13 with different AM^+ (Li^+, Na^+, and K^+). The cyclic voltammograms (CV) in the HER/HOR regime

show that the H_{upd} peak shows a clear dependence on the exact AM^+ (**Fig. 1a**). The peak potential is more positive in 0.1 M KOH and NaOH followed by 0.1 M LiOH (inset in **Fig. 1a**). A consistent and even more prominent trend has been previously observed on single crystal Pt surfaces by Koper and coworkers[7,25], in which H_{upd} peak was attributed not only to H adsorption but also to the replacement of OH_{ad} by H_{ad}[25]. **Thus, our work is in agreement with the previous reports that the negative peak shift with smaller AM^+ is an indication that Li^+ cations better stabilize (or less destabilize) OH_{ad} in the lower potential regime than Na^+ and K^+ cations.** Linear scan voltammograms (LSV) demonstrate the highest HER activity was observed in case of Li^+ followed by Na^+ and K^+ cations (**Fig. 1b**), also consistent with previous studies[16,26].

To understand the impact of these different AM^+ on the surface adsorbates in H_{upd}/HER regime, we have next exploited the ETS studies to directly probe the adsorbed species on the Pt surface. The ETS approach uses ultrafine PtNWs as a model catalyst[27,28], and involves a concurrent measurement of the PtNWs conductance during electrochemical studies at different electrochemical potentials (**Fig. 2a**). (See experimental section and ref [27] for detailed working principle of the technique). The PtNWs (~ 2nm diameter) used in ETS studies show qualitatively similar CV and LSV results (**Fig. S1**) with a consistent trend of AM^+ dependence to other types of Pt catalysts (e.g., Pt disc electrode).

Within the ETS approach, the electrical conductivity of ultrafine metallic PtNWs is sensitively dependent on the surface adsorbates due to surface adsorbate induced scattering of the conduction electrons, producing a resistance change following equations [27]:

$$\rho = \rho_0 \left(\left(\frac{1-p}{1+p} \right) \times \frac{\lambda}{d} \right) (d \ll \lambda)$$

Here ρ and ρ_0 are the resistivity of the one dimensional PtNWs and bulk metal respectively, λ is the mean free path of electron, d is the nanowire diameter, and p is a specularity parameter with a value ranging from 0 (for highly diffusive scattering) to 1 (completely specular scattering) (**Fig. 2b**)[29]. When the diameter (d) of the PtNWs is smaller than the electron mean free path (λ ~ 5 nm)[29], their resistance is highly dependent on the exact surface adsorbate that modifies the value of specularity (p). It is important to note such surface scattering is exclusively sensitive to surface adsorbates, with little impact for the electrostatic or electrochemical potential. For

example, previous studies have clearly shown a constant conductance at different electrochemical potentials when there is a stable surface adsorbate layer (*e.g.*, CO or I^-) that does not change with potential[27,28], clearly demonstrating the insensitivity of the metallic PtNWs to the varying electrochemical potentials. Thus, **the ETS approach offers a unique signal transduction pathway to exclusively probe the surface adsorbates, with minimum interferences from the electrochemical potentials or the bulk electrolyte environment, which is difficult to achieve with other analytic approaches that are often convoluted with near surface (e.g., EDL) or bulk electrolyte background.** Additionally, compared to interfacial-charge-transfer-based CV studies that cannot usually resolve surface adsorbates during active catalytic process (e.g., in HER potential regime) due to the dominance of much larger catalytic current over the surface adsorbate charge transfer, the ETS is exclusively sensitive to the surface adsorbates and insensitive to catalytic current. Thus, the ETS approach can allow to probe the surface adsorbates of active catalytic surfaces in action, which is essential for deciphering the catalytic molecular pathway.

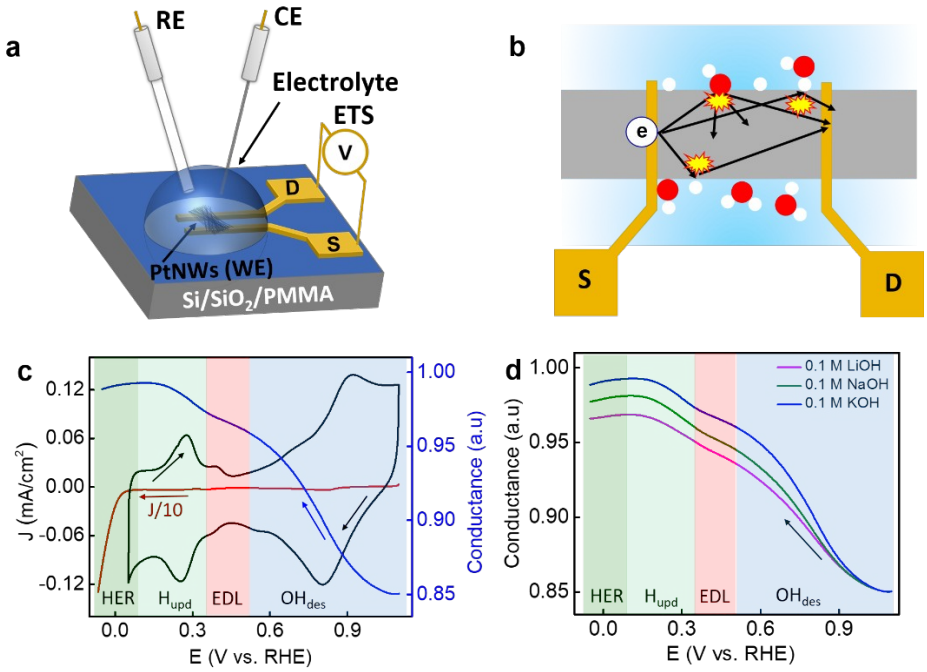

Figure 2| Schematic illustration of experimental setup and working principle of the on-chip electrical transport spectroscopy (ETS) measurements. (a) On-chip PtNW device for ETS measurements [RE, CE and PtNWs (WE) are reference, counter and Pt nanowires working electrodes respectively, S and D represents source and drain respectively] and **(b)** electrons scattering mechanism of various adsorbate molecules on PtNWs. **(c)** Typical cyclic voltammogram (black), negative sweeping branch to the HER

region (red) and the ETS spectra (blue). The red curve is divided by 10 due to much larger HER current in the HER protentional window. The OH_{des}, EDL, H_{upd} and HER regions are highlighted with different background color **(d)** Normalized ETS conductance signal versus potential of PtNWs device in 0.1 M MOH electrolyte solutions with different AM^+.

We have first closely compared the ETS measurement with the corresponding the CV curve when the potential is gradually changed from 1.10 - -0.05 V vs. reversible hydrogen electrode (RHE) (**Fig 2c**), which consistently shows four distinct regions: (i) $O/OH_{ad/des}$ region (1.10 - 0.60 V vs. RHE); (ii) electrical double layer region (OH_{ad} replaced by H_2O) (0.60 - 0.40 V vs. RHE); (iii) H_{upd} regime (0.40 - 0.08 V vs. RHE); and (iv) HER regime (0.08 - -0.05 V. RHE). The lowest conductance observed in the high potential regime is attributed to the larger scattering from the strongly bonded OH_{ad} on the Pt surface, which significantly reduces the conductance of the PtNWs. Scanning the potential toward lower potential regime results in a monotonic increase in conductance due to the gradual replacement of the OH_{ad} by H_2O. The conductance increase slowed in the double layer regime where Pt surface are nearly completely reduced and most of the OH_{ad} are replaced by H_2O. Further sweeping the potential to the more negative regime results in H_{upd} on electrode surface (replacement of surface adsorbed H_2O and residue OH_{ad} by H_{upd}), which further reduces scattering and increases conductance. The conductance eventually saturates at a nearly stable value below 0.15 V *vs.* RHE (beyond the H_{upd} peak in CV) due to a high coverage of adsorbed hydrogen. The ETS conductance measurement retains the nearly saturated conductance well into the HER regime (0.08 - -0.05 V vs. RHE), suggesting a largely similar surface adsorption status in the HER regime. The derivative of the ETS shows two peaks near the potential regime where most OH desorption and H-adsorption occurs, which is largely consistent with CV curve and further highlights the validity of our approach and analysis (**Fig. S2**).

We further compared the ETS data obtained with three different cations (Li^+, Na^+, and K^+). It was found the ETS data obtained with different cations show essentially the same conductance at high potential regime (1.10-1.00 V vs. RHE), suggesting a similar hydroxyl adsorption state at such potential. As we scan the potential towards lower potential regime, a notable conductance increase is observed in all cases, with a largely similar trend. However, it is interesting to note that the conductance increase is less pronounced with a smaller slope in the case of Li^+ cations as compared to that of Na^+ and K^+ (**Fig. 2d**). Considering the conductance increase is primarily

resulted from the replacement of OH_{ad} by H_2O and then by H_{upd}, the smaller increase in conductance in the presence of Li^+ cations suggests that less OH_{ad} are being desorbed or replaced by H_2O or H_{ad} when compared that with the other larger cations (Na^+ and K^+ cations). **We note that the difference among these three cations persist throughout the entire potential regime down -0.05V vs. RHE, suggesting different extent of OH_{ad} remained on the Pt in the H_{upd}/HER potential window.**

Theoretical insight into the role of cations on surface adsorbates

Although it has been commonly perceived that OH_{ad} may not be stable in the H_{upd}/HER potential regime, there are occasional suggestions that some level of OH_{ad} may persist in this potential regime[7,8], which is consistent with our ETS studies. To understand these experimental findings, we performed theoretical studies to investigate the extent of OH_{ad} in presence of different cations. To gain insight into how and why different cations influence the surface adsorption property, density functional theory (DFT) calculations are performed on the Pt(111)-water interface, which is modeled by the Pt(111) slab covered by an explicit water layer (**Fig. S3**). The DFT optimized geometries are shown in **Fig. S4**. The adsorption energy of OH_{ad} (E_{ad}^{OH}) on the Pt(111) is calculated to be -3.46 eV, -2.81 eV, and -2.32 eV (see below for the estimation of statistical fluctuations from solvent dynamics). in the presence of Li^+, Na^+, and K^+, respectively (**Fig. 3a**). Compared to the case of pure water environment (-3.50 eV), the presence of cations would destabilize the OH_{ad}, and the extent of such destabilization follows the trend of $K^+ > Na^+ > Li^+$. Grand canonical DFT calculations (**Fig. 3b**) confirm that this trend persists for potential-dependent adsorption free energy of OH (G_{ad}^{OH}) throughout the entire electrochemical window (-1.0 to 1.0 V vs. RHE), and the OH_{ad} is favorable even under a more negative potential.

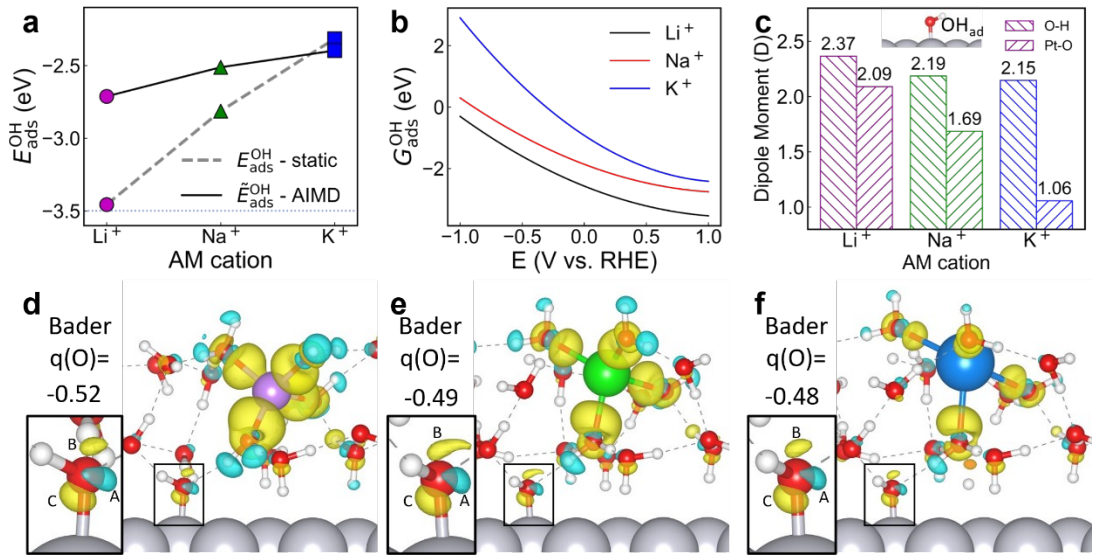

Figure 3| Effect of cations on adsorption of OH_{ad} at Pt(111)-water interface. (a) Adsorption energy of OH in presence of Li^+, Na^+, and K^+ ions, from static calculation and from AIMD simulation (statistical spread omitted here for clarity – see SI). The dotted horizontal line marks the adsorption energy in absence of any cation. **(b)** The potential-dependent G_{ad}^{OH} in presence of Li^+, Na^+, and K^+ ions in the potential window of 1.0 V to -1.0 V vs. RHE. **(c)** Bar plot showing the dipole moment of OH_{ad} based on Bader charges. The electron density difference map of Pt(111)-OH_{ad}-water interface after introducing **(d)** Li^+, **(e)** Na^+, and **(f)** K^+, plotted at the isovalue of 0.0025. Yellow and cyan isosurfaces represents spatial regions experiencing increase or decrease of electron density, respectively. The insets in (d-f) are zoomed-in views of the OH_{ad} regions, with key isosurfaces and Bader charges on O labeled.

Our DFT calculations show that the adsorption strength of OH_{ad} follows the order of Li^+ > Na^+ > K^+, which is consistent with the experimental observations in ETS studies (**Fig. 2d**). **To understand the origin of such difference in adsorption strength, we further calculated the electron density difference ($\Delta\rho_e$) at the Pt(111)-water interface after introducing different cations.** Overall, the interaction between the cation and the OH_{ad} is mostly electrostatic (decays in inverse square law) and its effect on the electronic structure of Pt surface is mild. **The yellow isosurfaces between cation and nearby water show the electron density redistribution on water to form cation-water bond, and a larger lobe suggests a higher extent of such redistribution (Fig. 3d-f). The more dramatic electron density redistribution in the presence of Li^+ can be attributed to the stronger local electric field from its highest charge density (same net charge but much smaller ionic radius), compared to Na^+ and K^+.** The electric field exerted by the cation also causes electron density redistribution in the OH_{ad}, reducing the electron density of the lone pair closest to the cation (region A in insets) while

increasing for the farther lone pair (region B in insets). **It is interesting to note that the region corresponding to Pt-O bond (region C in insets) also experiences an increase in electron density, which is due to charge compensation from bulk Pt to the polarized OH_{ad}.**

To further quantify such polarization and charge redistribution of OH_{ad}, we performed Bader charge analysis on the interface (**Fig. S5**), and the net charge on O in OH_{ad} is calculated to be -0.52 |e|, -0.49 |e|, and -0.48 |e| in presence of Li^+, Na^+, and K^+, respectively. **Based on Bader charges, the dipole moment of the O-H_{ad} (Pt-O) are calculated to be 2.37 D, 2.19 D, and 2.15 D (2.09 D, 1.69 D and 1.06 D) for Li^+, Na^+, and K^+ (Fig. 3c), respectively. Hence, it is clear that the extent of charge redistribution and polarization of OH_{ad} both follow the trend of $Li^+ > Na^+ > K^+$, which is likely caused by stronger electric field of Li^+, analogous to polarization of the first hydration sphere.**

Since the hydration sphere and water configuration at the Pt-water interface is not static, we further performed *ab initio* molecular dynamics (AIMD) simulations at the Pt(111)-water interface with near-surface hydrated cations in the canonical ensemble at 300 K to account for the dynamics and better sample the configurational space. A 100 ps trajectory is obtained for each system after pre-equilibration, with a variance of potential energy to be within 0.15 eV, marking proper equilibration of the system (**Fig. S6**). The cation-oxygen radial distribution function (RDF) (**Fig. S7**) obtained from the AIMD trajectory are consistent with the result of large-scale molecular mechanics (MM) simulation[23,30] and test simulations with a larger cell size or thicker water layer (Supplementary Note 1), demonstrating the correct hydration structure of the cations. The adsorption enthalpy (approximated by MD average of potential energy) of OH ($\widetilde{E}_{ad}^{OH}$) is calculated to be -2.71 eV, -2.51 eV, and -2.40 eV in presence of Li^+, Na^+, and K^+, respectively (**Fig. 3a**), which is largely consistent with the trend of the E_{ad}^{OH} and potential-dependent G_{ad}^{OH} calculated for static models (**Fig. 3a,b**), further confirming more favorable OH_{ad} in the presence of Li^+.

The reduction of the adsorption energy (**Fig. 3a**) with increasing AM^+ size (from Li^+, Na^+, to K^+) is contributed by the interface dynamics. We note it has been a debated topic whether cations directly adsorb or simply accumulate in the outer-Helmholtz plane in the double layer[31-33]. Hence, we further studied the cation dynamics and its hydration structure. The representative

snapshot of each system at equilibrium and at the position closest to the surface (**Fig. S8**) shows that the cation stays in the double layer most of the time, oscillating between the first and second water layers. During the 100 ps AIMD simulation, Li^+ maintains a coordination number (CN) of 4 and oscillates in the upper half between the first and second water layer. The CN fluctuates between 4 and 5 for Na^+ and oscillates in the lower half between the first and second water layer. On the other hand, K^+ doesn't have a specific CN, and frequently penetrates the first water layer but never stays specifically adsorbed on the Pt surface. The cation coordination numbers (4 for Li^+, ~4-5 for Na^+, ~4-6 for K^+) obtained in our simulation are consistent with ref[34], and the position of cations is consistent with ref[33]. The averaged distance between the cation and Pt(111) surface are 4.44 Å, 4.42 Å, and 3.95 Å without surface OH and 5.38 Å, 4.43 Å, and 3.88 Å with surface OH, respectively, which is due to different rigidness of their hydration sphere as also characterized by the sharpness of RDF peak (**Fig. S7**). Notably, only Li^+ is observed to have a well-defined second hydration sphere, and only K^+ experiences instantaneous penetration of water inside its first hydration shell (**Fig. S7**). The variation in cation-surface distance partially smears the difference in OH adsorption for different cations, while leaving the overall trend qualitatively unchanged. The distinct interfacial dynamics are attributed to the different charge density of the cations, cation-water interaction strength, and the mass of the cations (heavier cations are less dragged by the friction of its water environment). It is noted that the observation that the cations do not stay dehydrated and form bonds with the Pt surface contradicts the hypothesis previously proposed in ref[7,32,35,36], whose discrepancy is likely a result of undercoordination of the cations from insufficient explicit solvation, which leads to the overestimation of cation-surface binding strength. We also note that previous studies indicated large cations (e.g., Cs^+) may show a stronger interaction and direct adsorption on electrode surface due to less tightly bounded solvation shell in large cations[26]. Indeed, our preliminary ETS studies also suggested that the larger cations (Rb^+ or Cs^+) may directly adsorb on electrode surface (Supplementary Note 2) and are expected to influence the HER activity in a very different way. Therefore, we excluded the Rb^+ and Cs^+ ions from this study.

Cation modulation of local chemical environment and HER kinetics

The aforementioned experimental ETS results and theoretical calculations confirm that the AM^+ don't specifically adsorb on the electrode surface but instead accumulate in outer-Helmholtz plane. To probe the distribution of cations in the outer-Helmholtz plane of the EDL, we performed electrochemical impedance spectroscopy (EIS) analysis in different cation electrolytes and determined the double layer capacitance (C_{dl}) at different applied potentials (**Fig. 4a**). In the simplified equation, the C_{dl} is directly related to the relative permittivity (ε) of the solvent at constant electrolyte concentration (C) as shown below [37].

$$C_{dl} = \varepsilon \varepsilon_o \sqrt{C}$$

The EIS studies reveal a larger C_{dl} in the high potential regime (1.1-0.6 V vs. RHE) for K^+ than for Na^+ and Li^+, which can be attributed to lower hydration energy, shorter cation-surface distance, and less rigid hydration sphere (hence a smaller effective hydration sphere radius) of K^+ as compared to Na^+ and Li^+ [38]. However, an opposite trend was observed when the potential goes into H_{upd}/HER regime, showing a larger C_{dl} in case of Li^+. **This reversal in C_{dl} is attributed to the change in local cation concentration induced by the change in surface species.** With the interaction between hydrated cation and surface OH_{ad} shown in our DFT calculations, we hypothesize that local cation concentration might be highly dependent on the coverage and polarity of surface OH_{ad}, and might be substantially different from the bulk concentration.

To further explore how the surface OH_{ad} and near-surface cations influence the dynamic properties of each other, we analyze the AIMD trajectories of Pt(111)-water and Pt(111)-OH_{ad}-water with near-surface hydrated cations. **The first peak in RDF of Pt-O (Fig. 4b) corresponds to Pt-OH bond, and is the leftmost and sharpest in presence of Li^+ followed by Na^+ and K^+, suggesting the strongest Pt-OH bond with Li^+ and consistent with experimental and theoretical results discussed in the previous sections.** The second peak corresponds to the first water layer, and it is about the same for three cations, showing consistent distribution of near-surface water independent on identity of the hydrated cations.

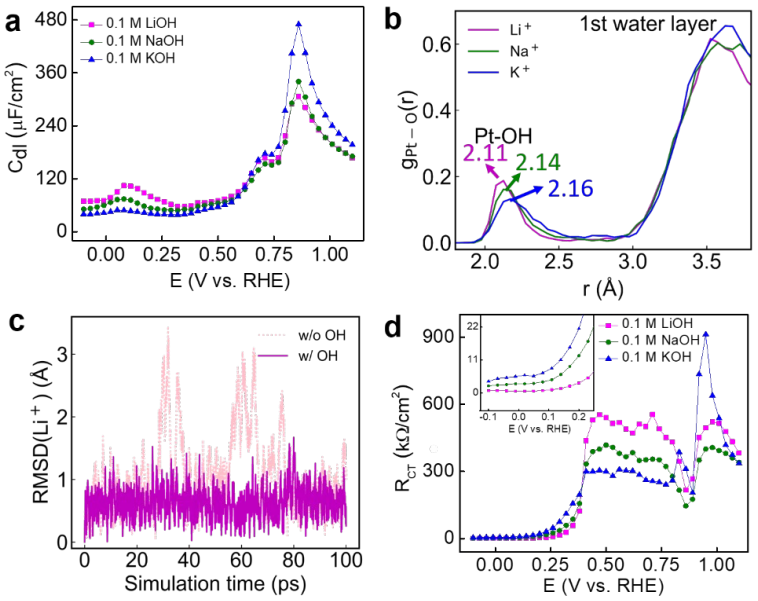

Figure 4| EIS and DFT investigation of role of adsorbed hydroxides in stabilizing the cations in the electrical double layer region and their role in decreasing the charge transfer resistance. (a) Double layer capacitance (C_{dl}) on Pt disc electrode at different applied potentials in 0.1 M MOH solutions (M= Li^+, Na^+ and K^+) **(b)** The radial distribution function $g_{Pt-O}(r)$ between Pt and O atoms in the Pt(111)-OH_{ad}-water interface in presence of Li^+, Na^+, and K^+ ions calculated from AIMD trajectory. **(c)** The root mean square deviation of the position of Li^+, with and without OH_{ad} on the Pt surface, during the 100 ps AIMD simulation. **(d)** Charge transfer resistance (R_{ct}) on Pt disc electrode at different applied potentials in 0.1 M MOH solutions (M= Li^+, Na^+ and K^+).

Interestingly, the polarized OH_{ad} in turn could stabilize the hydrated cations to stay in its surrounding. The root-mean square deviation (RMSD) of the Li^+ position from the Pt surface shows considerably larger fluctuation in absence of OH_{ad} (**Fig. 4c**), suggesting large and frequent oscillation and drifting of Li^+ away from its equilibrium position (zero reference). After introducing OH_{ad}, the RMSD flattens and seldom goes beyond 1.5 Å from the equilibrium position, suggesting an "anchoring" of Li^+ cations to the Pt surface by OH_{ad}. A similar "anchoring" effect is also observed for Na^+ and K^+ ions, although to a less extent due to weaker cation-OH interactions (**Fig. S9**). We note such anchoring differs from the specific adsorption since the cation and OH_{ad} is separated by the first hydration shell (ca. 4 Å apart) without forming any direct cation-OH bond or OH_{ad}-induced dehydration (Supplementary Note 3), which differs from the work by Koper and Janik despite a similar trend [7,8]. Since the OH_{ad} has the higher surface coverage and polarity in presence of Li^+ followed by Na^+ and K^+, which means more

anchors and stronger anchoring effect, leading to a higher local concentration of cations (Li^+ > Na^+ > K^+) near the Pt surface.

To conclude, the crossover of C_{dl} in the EIS near 0.60 V vs. RHE is induced by the change in surface coverage of OH_{ad}: (1) at higher potential (>0.60 V vs. RHE) where there are abundant surface OH_{ad}, the capacitance (K^+ > Na^+ > Li^+) is more determined by the inverse of cation-surface distance and hydration sphere size; (2) at lower potential (<0.60 V vs. RHE) when there is only a limited number of OH_{ad}, the capacitance (Li^+ > Na^+ > K^+) is more dictated by the local cation concentration which is in turn related to coverage of the remaining OH_{ad} due to its anchoring effect.

The charge transfer resistance was also determined from EIS data. The electrode-electrolyte interface was largely capacitive in the entire potential range except the HER region (**Fig. 4d**). The charge transfer resistance is the opposition experienced for electron movement at electrode-electrolyte interface. The charge transfer resistance in the oxidation region (~1V) is not meaningful as it is largely capacitive with a minimal charge transfer process. **However, in the hydroxyl desorption potential regime (~0.9-0.4V vs. RHE), the charge transfer resistance is larger for Li^+ ions when compared to Na^+ and K^+ ions, suggesting more difficult desorption of OH_{ad} and replacement by H_2O molecules in presence of Li^+ ions, consistent with our ETS results.** While in the H_{upd} and HER regime (<0.4 V vs. RHE), the charge transfer resistance is lowest for Li^+ ions followed by Na^+ and K^+ ions, consistent with the improved Volmer step kinetics for H_{upd} and HER for Li^+ ions followed by Na^+ and K^+ ions **(Fig. 1b)**.

To further understand the HER activity trend, we focus on the behavior of water molecules in the AIMD because water is the major proton source in alkaline HER. With the alkaline Volmer step (involving water dissociation) being the rate determining step [13], the O-H bond strength in near-surface water could work as a metric explaining HER activity. To this end, we examined the RDF of O-H of water in the surrounding of different species (**Fig. 5a)**. Compared to the water in the regular bulk water environment, the water O-H bond length in the first hydration shell of cation experiences a downshift of the peak position and a slight sharpening of the peak, suggesting the strengthening of the O-H bond of water in the hydration shell of cations. **On the other hand, the O-H peak of water molecules next to both O and H of OH_{ad} show a**

longer tail on the stretching side (~1.05 - 1.1 Å), indicating that OH_{ad} can function as both proton acceptors and donors to weaken O-H bond in nearby water, hence leading to a lower barrier for water dissociation.

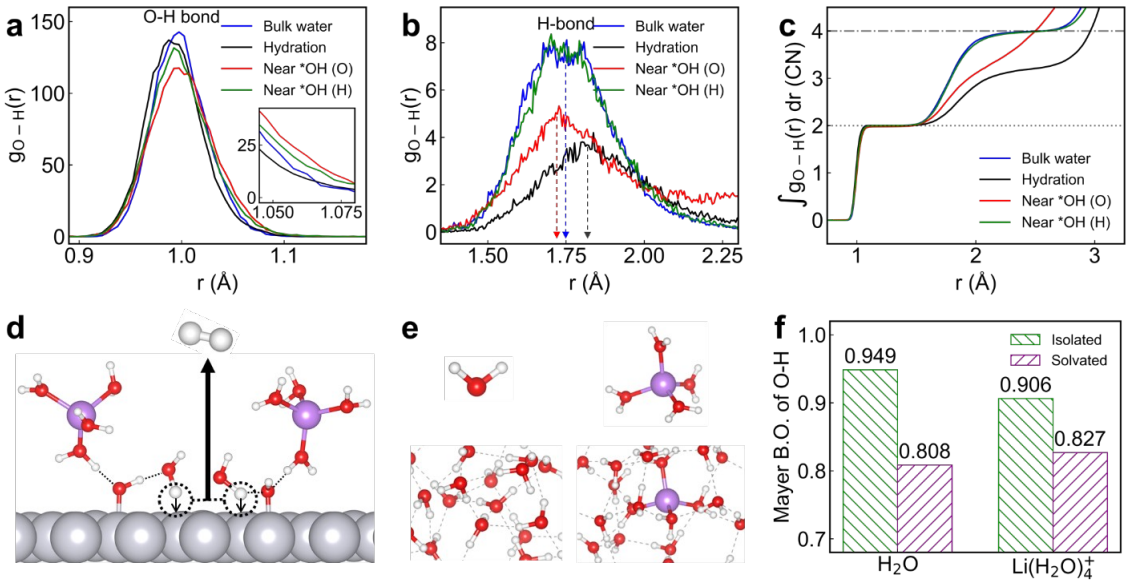

Figure 5| AIMD and micro-solvation simulation on the role of cation and OHad on reactivity of nearby water. The radial distribution function $g_{O-H}(r)$ between O and H atoms in the Pt(111)-OH_{ad}-water interface in presence of Li^+ in **(a)** covalent O-H region and **(b)** non-covalent O…H H-bond region. The decomposed curves belong to water molecules in the hydration sphere of Li^+, in the bulk water, or near the surface OH_{ad} as its H-bond donor or acceptor. Inset in (a) shows zoomed-in view of the tail region corresponding to O-H stretching. **(c)** Integrated $g_{O-H}(r)$ showing the coordination number (CN) of O by H at different r(O-H) distances, with dotted and dash-dot lines marking CN=2 and CN=4, respectively. **(d)** Schematics showing the promotion of alkaline Volmer step by surface OH_{ad} at the Pt(111)-water interface. **(e)** Optimized geometry of H_2O and $Li(H_2O)_4^+$ in isolated state (top row) or in solvated state (bottom row). **(f)** Bar chart of the Mayer bond order of O-H in H_2O and $Li(H_2O)_4^+$ in isolated state or in solvated state.

The variation of water reactivity near different species can also be partly explained by different H-bond strength with their environment, which is characterized by the H-bond peak in the O···H RDF. The earlier and sharper peaks in the r ~1.5-2.0 Å region (**Fig. 5b**) suggest stronger and more directional H-bond interaction on the water molecules by its environment. Compared to the bulk water case (peak position at c.a. 1.76 Å), the water in the first hydration shell of cation has a broader shape and later peak position (c.a. 1.80 Å) due to the blockage/restraint of H-bond formation by steric of the cation and the hydration shell. It is interesting to note the water molecules near the O in OH_{ad} show a shorter H-bond peak (c.a. 1.73

Å), indicating considerably strengthened H-bond, which is fundamentally originated from highly polar OH_{ad} with a much higher negative charge density on O atoms than that in near-surface water, as evidenced by the Bader charges (-0.52 |e| on O in OH_{ad} *vs.* c.a. -0.2 |e| on O in near-surface water) (**Fig. S5a**). **These analyses indicate that OH_{ad} functions as strongly polarized H^+-acceptors for nearby water molecules and thus facilitate water dissociation.** The peak area, which corresponds to the coordination number of O by H (**Fig. 5c**), is smaller than the case of bulk water probably due to blockage of H-bond sites by the steric hindrance of the Pt surface.

The water near the H in OH_{ad} (with OH_{ad} being H-bond donor) has a similar peak height/area to that in bulk water (**Fig. 5b**), indicating a similar hydrogen bond strength. The Bader charge analysis indicates that there is less positive charge on H in OH_{ad} (0.04 |e| for H in OH_{ad} *vs.* ~ 0.1 |e| on H in water), the surface OH_{ad} is thus an electronically weaker H-bond donor. On the other hand, the longer tail in the O-H stretching region for water near H in OH_{ad} (**Fig. 5a inset**) indicates the OH_{ad} does function as a proton donor to weaken O-H in nearby water molecules, which is likely due to synergistic geometric effect of the surface bound OH_{ad} and near Pt-surface water dynamics.

Together, by combining systematic experimental and theoretical studies, we reveal that that **the cations play an indirect role in alkaline HER on Pt**. It is the enhanced surface concentration of OH_{ad} induced by presence of smaller cations (Li^+), instead of the cation itself, that enhances the HER activity in alkaline media (**Fig. 5d).** The smaller cations lead to a higher OH_{ad} coverage on Pt surface in the HER potential window, which can act as **an electronically favored proton acceptors and geometrically favored proton acceptors to promote water dissociation and the Volmer step kinetics in alkaline media**. The higher OH_{ad} coverage in case of Li^+ ions (followed by Na^+ and then K^+) leads to the higher HER activity.

We note in our finding that cations stabilize its first hydration shell is to the very contrary of the common perception that the cations can directly activate its hydration sphere [35,39], and hence we performed a sanity check with a finer micro-solvation model at a higher level of theory and evaluated Mayer bond order (BO) of the O-H bonds based on DFT-optimized geometries (**Fig. 5e,f**). Without explicit solvation, the Mayer bond order of H-O in the hydration shell of Li^+ (0.906) is lower than that of an isolated water (0.949), resulting from

polarization by the electrostatics of the cation. Interestingly, the trend is reversed when the system is subject to explicit solvation. In a H-bond network, each water molecule is connected to four neighboring water molecules via H-bond, which causes a significant weakening of the O-H bond in water to result in a Mayer BO of 0.808. However, each water molecule in the first hydration shell of Li^+ can only connect to 2 or 3 neighboring water molecules due to the blockage of H-bond sites by the steric effect of the cation. **The Mayer bond order of the O-H in the hydration shell of cation (0.827) is therefore weakened to a lesser extent since the effect of water environment outcompetes the effect of cations. In other words, the water in the hydration shell of cation is stabilized compared to the water in bulk water.** Hence, the argument of "*cation activating its hydration sphere*" is likely a victim of underestimating the role of the water environment. We recognize that the models adopted in this study have certain limitations in various aspects due to computation-cost limitations (see details in Supplementary Note 4), we believe this example well highlights the necessity of including sufficient explicit solvation to properly describe the reactivity of water both in bulk solution and at an electrochemical interface.

Summary

In conclusion, we have combined a unique surface-adsorbate exclusive electrical transport spectroscopy (ETS) approach with the electrochemical impedance spectroscopy (EIS) and DFT calculations to directly probe the on-surface and near-surface chemical environment, deciphering the elusive role of AM^+ on Pt surface chemistry and alkaline HER. Our integrated studies suggests that the cation is not directly bonded to the Pt surface or OH_{ad}, but separated by a water molecule in the first hydration shell of the cation, distinct from previous studies[7]; and that smaller cations favor higher OH_{ad} coverage on Pt surface in the HER potential window, which in turn function as electronically favored proton acceptors or geometrically favored proton donors to promote water dissociation and the Volmer step kinetics on Pt surface in alkaline media, leading to improved HER activity in the presence of smaller cations (Li^+). Our studies resolve the fundamental role of AM^+ in HER kinetics that has remained elusive in recent decades, and could offer valuable insights for the design more efficient electrolyzers for renewable energy conversion.

References

1 Sheng, W., Gasteiger, H. A. & Shao-Horn, Y. Hydrogen oxidation and evolution reaction kinetics on platinum: acid vs alkaline electrolytes. *J. Electrochem. Soc.* **157**, B1529-B1536 (2010).

2 Li, L., Wang, P., Shao, Q. & Huang, X. Recent Progress in Advanced Electrocatalyst Design for Acidic Oxygen Evolution Reaction. *Adv. Mater*. **33**, 2004243-2004266, (2021).

3 Gasteiger, H. A., Panels, J. E. & Yan, S. G. Dependence of PEM fuel cell performance on catalyst loading. *J. Power Sources.* **127**, 162-171 (2004).

4 Nørskov, J. K. *et al.* Trends in the exchange current for hydrogen evolution. *J. Electrochem. Soc.* **152**, J23-J26 (2005).

5 Zhang, W. et al. WO_x-Surface Decorated PtNi@Pt Dendritic Nanowires as Efficient pH-Universal Hydrogen Evolution Electrocatalysts. *Adv. Energy Mater.* **11**, 2003192-2003198 (2021).

6 Sheng, W., Myint, M., Chen, J. G. & Yan, Y. Correlating the hydrogen evolution reaction activity in alkaline electrolytes with the hydrogen binding energy on monometallic surfaces. *Energy Environ. Sci.* **6**, 1509-1512 (2013).

7 Chen, X., McCrum, I. T., Schwarz, K. A., Janik, M. J. & Koper, M. T. M. Co-adsorption of Cations as the Cause of the Apparent pH Dependence of Hydrogen Adsorption on a Stepped Platinum Single-Crystal Electrode. *Angew. Chem. Int. Ed.* **56**, 15025-15029 (2017).

8 McCrum, I. T., Chen, X., Schwarz, K. A., Janik, M. J. & Koper, M. T. M. Effect of Step Density and Orientation on the Apparent pH Dependence of Hydrogen and Hydroxide Adsorption on Stepped Platinum Surfaces. *J. Phys. Chem. C.* **122**, 16756-16764 (2018).

9 Ledezma-Yanez, I. *et al.* Interfacial water reorganization as a pH-dependent descriptor of the hydrogen evolution rate on platinum electrodes. *Nat. Energy.* **2**, 1-7 (2017).

10 Seto, K., Iannelli, A., Love, B. & Lipkowski, J. The influence of surface crystallography on the rate of hydrogen evolution at Pt electrodes. *J. Electroanal. Chem. Interf. Electrochem.* **226**, 351-360 (1987).

11 Markovića, N. M., Sarraf, S. T., Gasteiger, H. A. & Ross, P. N. Hydrogen electrochemistry on platinum low-index single-crystal surfaces in alkaline solution. *J. Chem. Soc. Faraday Trans.* **92**, 3719-3725 (1996).

12 Marković, N., Grgur, B. & Ross, P. N. Temperature-dependent hydrogen electrochemistry on platinum low-index single-crystal surfaces in acid solutions. *J. Phys. Chem. B.* **101**, 5405-5413 (1997).

13 Subbaraman, R. *et al.* Enhancing Hydrogen Evolution Activity in Water Splitting by Tailoring Li^+-$Ni(OH)_2$-Pt Interfaces. *Science* **334**, 1256-1260 (2011).

14 Subbaraman, R. *et al.* Trends in activity for the water electrolyser reactions on 3d M(Ni,Co,Fe,Mn) hydr(oxy)oxide catalysts. *Nat. Mater.* **11**, 550-557 (2012).

15 Li, J. *et al.* Experimental Proof of the Bifunctional Mechanism for the Hydrogen Oxidation in Alkaline Media. *Angew. Chem. Int. Ed.* **56**, 15594-15598 (2017).

16 Liu, E. *et al.* Unifying the Hydrogen Evolution and Oxidation Reactions Kinetics in Base by Identifying the Catalytic Roles of Hydroxyl-Water-Cation Adducts. *J. Am. Chem. Soc.* **141**, 3232-3239 (2019).

17 Cong, Y. *et al.* Uniform $Pd_{0.33}Ir_{0.67}$ nanoparticles supported on nitrogen-doped carbon with remarkable activity toward the alkaline hydrogen oxidation reaction. *J. Mater. Chem. A.* **7**, 3161-3169 (2019).

18 Qiu, Y. *et al.* BCC-Phased PdCu Alloy as a Highly Active Electrocatalyst for Hydrogen Oxidation in Alkaline Electrolytes. *J. Am. Chem. Soc.* **140**, 16580-16588 (2018).

19 McCrum, I. T. & Koper, M. T. M. The role of adsorbed hydroxide in hydrogen evolution reaction kinetics on modified platinum. *Nat. Energy*. **5**, 891-899 (2020).

20 Xue, S. *et al.* Influence of Alkali Metal Cations on the Hydrogen Evolution Reaction Activity of Pt, Ir, Au, and Ag Electrodes in Alkaline Electrolytes. *ChemElectroChem.* **5**, 2326-2329 (2018).

21 Monteiro, M. C. O., Goyal, A., Moerland, P. & Koper, M. T. M. Understanding Cation Trends for Hydrogen Evolution on Platinum and Gold Electrodes in Alkaline Media. ACS Catal. 11, 14328-14335 (2021).

22 Weber, D., Janssen, M. & Oezaslan, M. Effect of monovalent cations on the HOR/HER activity for Pt in alkaline environment. *J. Electrochem. Soc.* **166**, F66-F73 (2019).

23 Intikhab, S., Snyder, J. D. & Tang, M. H. Adsorbed Hydroxide Does Not Participate in the Volmer Step of Alkaline Hydrogen Electrocatalysis. *ACS Catal.* **7**, 8314-8319 (2017).

24 McCrum, I. T. & Koper, M. T. M. The role of adsorbed hydroxide in hydrogen evolution reaction kinetics on modified platinum. *Nat. Energy.* **5**, 891-899, (2020).

25 van der Niet, M. J. T. C., Garcia-Araez, N., Hernández, J., Feliu, J. M. & Koper, M. T. M. Water dissociation on well-defined platinum surfaces: The electrochemical perspective. *Catal. Today* **202**, 105-113 (2013).

26 Huang, B. *et al.* Cation- and pH-Dependent Hydrogen Evolution and Oxidation Reaction Kinetics. *JACS Au.* **1**, 1674-1687 (2021).

27 Ding, M. *et al.* An on-chip electrical transport spectroscopy approach for in situ monitoring electrochemical interfaces. *Nat. Commun.* **6**, 1-9 (2015).

28 Ding, M. *et al.* On-chip in situ monitoring of competitive interfacial anionic chemisorption as a descriptor for oxygen reduction kinetics. *ACS Cent. Sci.* **4**, 590-599 (2018).

29 Yoo, H.-W., Cho, S.-Y., Jeon, H.-J. & Jung, H.-T. Well-Defined and High Resolution Pt Nanowire Arrays for a High Performance Hydrogen Sensor by a Surface Scattering Phenomenon. *Anal. Chem.* **87**, 1480-1484 (2015).

30 Kiyohara, K. & Minami, R. Hydration and dehydration of monovalent cations near an electrode surface. J. Chem. Phys. **149**, 014705-014714 (2018).

31 Rebollar, L. *et al.* "Beyond Adsorption" Descriptors in Hydrogen Electrocatalysis. *ACS Catal.* **10**, 14747-14762 (2020).

32 Mills, J. N., McCrum, I. T. & Janik, M. J. Alkali cation specific adsorption onto fcc(111) transition metal electrodes. *Phys. Chem. Chem. Phys.* **16**, 13699-13707 (2014).

33 Ringe, S. *et al.* Understanding cation effects in electrochemical CO_2 reduction. *Energy Environ. Sci.* **12**, 3001-3014 (2019).

34 Mähler, J. & Persson, I. A Study of the Hydration of the Alkali Metal Ions in Aqueous Solution. *Inorg. Chem.* **51**, 425-438 (2012).

35 McCrum, I. T. & Janik, M. J. First Principles Simulations of Cyclic Voltammograms on Stepped Pt(553) and Pt(533) Electrode Surfaces. *ChemElectroChem.* **3**, 1609-1617 (2016).

36 McCrum, I. T. & Janik, M. J. pH and Alkali Cation Effects on the Pt Cyclic Voltammogram Explained Using Density Functional Theory. *J. Phys. Chem. C.* **120**, 457-471 (2016).

37 Lust, E. Electrical Double Layers. Double Layers at Single-crystal and Polycrystalline Electrodes. *In Encyclopedia of Electrochemistry*; Bard, A. J., Eds., Wiley, 2002.

38 Garlyyev, B., Xue, S., Watzele, S., Scieszka, D. & Bandarenka, A. S. Influence of the Nature of the Alkali Metal Cations on the Electrical Double-Layer Capacitance of Model Pt(111) and Au(111) Electrodes. *J. Phys. Chem. Lett.* **9**, 1927-1930 (2018).

39 Goyal, A. & Koper, M. T. Understanding the role of mass transport in tuning the hydrogen evolution kinetics on gold in alkaline media. *J. Chem. Phys.* **155**, 134705-134715 (2021).

Data availability

The data that support the plots within this paper and other findings of this study are available from the corresponding author upon reasonable request.